Materials Science and Engineering C 78 (2017) 842–846

Contents lists available at ScienceDirect

Materials Science and Engineering C

journal homepage: www.elsevier.com/locate/msec

Solvothermal synthesis of cobalt ferrite hollow spheres with chitosan

Sarah Briceño [a,b,*], Jorge Suarez [a], Gema Gonzalez [a,c]

[a] Laboratorio de Materiales, Centro de Ingeniería de Materiales y Nanotecnología, Instituto Venezolano de Investigaciones Científicas (IVIC), Apartado 20632, Caracas 1020-A, Venezuela
[b] Yachay Tech University, School of Physical Sciences and Nanotechnology, 100119-Urcuquí, Ecuador
[c] Dpto. Física, Escuela Politécnica Nacional, Quito, Ecuador

ARTICLE INFO

Article history:
Received 7 October 2016
Received in revised form 4 April 2017
Accepted 6 April 2017
Available online 27 April 2017

Keywords:
Chitosan
Ferrite
Nanoparticle
Hollow sphere
Magnetic properties

ABSTRACT

Cobalt ferrite hollow spheres with chitosan ($CoFe_2O_4$/CS) were synthesized by two different approaches using the solvothermal method. The first approach involves in-situ incorporation of $FeCl_3$:$6H_2O$ and $CoNO_3$:$6H_2O$ in the solvothermal reaction (M1) and in second approach already prepared $CoFe_2O_4$ nanoparticles (NPs) using the thermal decomposition method was placed in the solvothermal reaction to form the hollow spheres (M2). Structural identification of the samples were characterized by Fourier transform infrared spectra (FTIR), powder X-ray diffraction (XRD), scanning electron microscopy (SEM), transmission electron microscopy (TEM), thermogravimetric analyses (DSC-TGA) and energy dispersive X-ray spectroscopy (EDX). The magnetic properties were evaluated using a vibrating sample magnetometer (VSM). The presence of chitosan on the hollow sphere was confirmed by FTIR. The XRD analyses proved that the synthesized samples were cobalt ferrite with spinel structure. The structure of the surface and the average particle size of the spheres were observed by SEM and TEM showing the nano scale of the $CoFe_2O_4$ component. Structural characterization demonstrating that chitosan does not affect the crystallinity, chemical composition, and magnetic properties of the $CoFe_2O_4$/CS. This work demonstrates that the $CoFe_2O_4$/CS prepared using the as synthesized $CoFe_2O_4$ NPs have better structural and magnetic properties.

1. Introduction

Magnetic chitosan hollow spheres are rather cheap, non-toxic, alkali resistant, corrosion resistant, easily degradable, easily recyclable, and with potential applications in catalysts, chemical sensors, drug delivery [1], photonic crystal, low-density structural materials and in biotechnology [2]. Structural and magnetic properties of hollow spheres are given by their chemical composition, size and shape. Those materials usually reveal special properties in addition to the individual contributions [3,4]. Therefore, preparation of hollow nanomaterials with controllable crystal structure and morphology gets great attention. Numerous synthetic techniques have been explored including chemical co-precipitation [5], thermal decomposition [6] and hydrothermal or solvothermal [7] methods and, in addition, methods utilizing templates in order to obtain hollow structures [8]. However, controllable preparation of nanostructures with desired size, shape and magnetic properties and functionalizable surface in a one-step simple and low cost method presents still a great challenge. For biomedical applications, chitosan-coated magnetic hollow spheres are generally synthesized by in situ coating method which is alkaline coprecipitation of Fe(II) and Fe(III) precursors in aqueous solutions of hydrophilic chitosan polymers. These polymers serve to limit the core growth of iron oxide during the preparation, to stabilize via steric repulsions when the nanoparticles disperse in aqueous media, and to reduce the opsonization process in vivo [9]. Several works [2,10], have been reported in the synthesis of hollow nanomaterials, however the optimization of the structural and magnetic properties still remains a challenge. In the present work, we report the influence of the preparation method on the morphology and magnetic properties of cobalt ferrite hollow spheres with chitosan using a simple solvothermal process with $CoFe_2O_4$ nanoparticles previously prepared by the thermal decomposition method and the formation of the $CoFe_2O_4$ nanoparticles in-situ in the solvothermal reaction with a ferrous precursor and their characterization by IRFT, XRD, SEM, TEM, TGA and magnetic measurements. The great advantage of the present work compared with those previously reported [11] is that the magnetic properties of the hollow spheres can be optimized by controlling the size of the nanoparticles previously formed by the thermal decomposition method.

2. Experimental

$CoFe_2O_4$/CS hollow spheres were prepared using the same solvothermal procedure but in two different ways; in-situ and ex-situ incorporation of $CoFe_2O_4$NPs into the chitosan (CS).

* Corresponding author at: Laboratorio de Materiales, Centro de Ingeniería de Materiales y Nanotecnología, Instituto Venezolano de Investigaciones Científicas (IVIC), Apartado 20632, Caracas 1020-A, Venezuela.
E-mail address: sbriceno@ivic.gob.ve (S. Briceño).

http://dx.doi.org/10.1016/j.msec.2017.04.034
0928-4931/

2.1. In-situ synthesis of $CoFe_2O_4$/CS hollow spheres (M1)

In-situ incorporation of $CoFe_2O_4$ NPs was done by adding 1.60 g of $FeCl_3$:$6H_2O$, 0.8 g of $CoNO_3$:$6H_2O$, 2.5 g of chitosan, 3.6 g of NaOAc and 1.0 g of PVP to 50 mL of ethylene glycol to give a transparent solution. This mixture was then transferred to a Teflon-lined autoclave (80 mL) for treatment at 250 °C for 13 h. Finally, ethanol was added to the samples, separated via centrifugation and dried in an oven at 60 °C for further use.

2.2. Ex-situ synthesis of $CoFe_2O_4$/CS hollow spheres (M2)

In this process the $CoFe_2O_4$ ferrite NPs were prepared separately by the thermal decomposition method [6]. The procedure consisted on mixing $Fe(acac)_3$, $Co(acac)_3$, 1,2 hexadecanediol, oleic acid, oleylamine and benzyl ether. The nuclei formation and the growth of the Nps were obtained when temperature was increased to 200 °C for 30 min with argon and heated to reflux at 265 °C for another 30 min. Ex-situ incorporation of previously prepared $CoFe_2O_4$ NPs was done by adding 1.0 g of $CoFe_2O_4$ NPs, 2.5 g of chitosan, 3.6 g of NaOAc and 1.0 g of PVP to 50 mL of ethylene glycol to give a transparent solution. This mixture was then transferred to a Teflon-lined autoclave (80 mL) for treatment at 250 °C for 13 h. Finally, ethanol was added to the samples, separated via centrifugation and dried in an oven at 60 °C for further use.

2.3. Characterization

The crystal structure of the samples was identified by X-ray powder diffraction performed in a Bruker D8-Focus X-ray diffractometer (XRD) equipped with parallel beam geometry and Cu K radiation ($\lambda = 1.5406$ Å), operated by DifraccPlus software with a voltage of 40 kV, current of 30 mA and angles ranged from 5 to 90° in 0.020 steps. Infrared spectra were recorded using a Perkin Elmer model 1650 FT-IR spectrometer between 4000 and 250 cm^{-1}. SEM analysis was performed in a FEI Inspect F50 scanning electron microscope, working with an acceleration voltage of 8–10 keV, attached with energy dispersive X-ray microanalysis, EDAX 8500 (silicon drift detector (SSD)). TEM analysis was carried out in a FEI spirit instrument (120 Kv) electron microscope. The thermal properties were studied using SDT Q600 simultaneous DSC - TGA thermogravimetric system. Hysteresis loops with a maximum field of 1T were measured in a Vibrating Sample Magnetometer Varian Techtron 155 at room temperature.

3. Results and discussion

3.1. Fourier transform infrared (FTIR)

The bonding between chitosan and $CoFe_2O_4$ NPs of the samples M1 and M2 was confirmed by FTIR measurements in the Fig. 1. The characteristic band of the intrinsic Fe—O stretching of the spinel structure is observed between 560 and 590 cm^{-1} for both samples, corresponding to vibrations of the metal at the tetrahedral site. In the range of 370–410 cm^{-1} are the Fe—O stretching vibrations of the octahedral site [5]. The peaks at around 897 and 1159 cm^{-1} are assigned to the saccharide structure of the chitosan, and its C—O—C functional groups are found at 1052 and 1071 cm^{-1}. The characteristic bands of amide I, amide II, and amide III for CS can be found at 1658, 1596, and 1380 cm^{-1}, respectively. The peak at 1546 cm^{-1} is attributed to the —NH deformation vibration of the amine groups belonging to CS [12]. For the M2 sample, additionally, two characteristic bands are observed at 2923 cm^{-1}, corresponding to asymmetric and symmetric stretching of C—H bonds of the aliphatic chain, these absorptions suggest that the NPs prepared by the thermal decomposition method are coated with oleic acid [13]. In the spectra of the sample M2, it is apparent that the absorption line at 1158 cm^{-1} and the amide absorptions became relatively larger than those in the sample M1. This fact indicates that there was strong hydrogen bonding between the oxygen in $CoFe_2O_4$ and the hydrogen in the amino group (—NH_2) in chitosan, which explains the larger amide absorptions in the spectra of the sample M2.

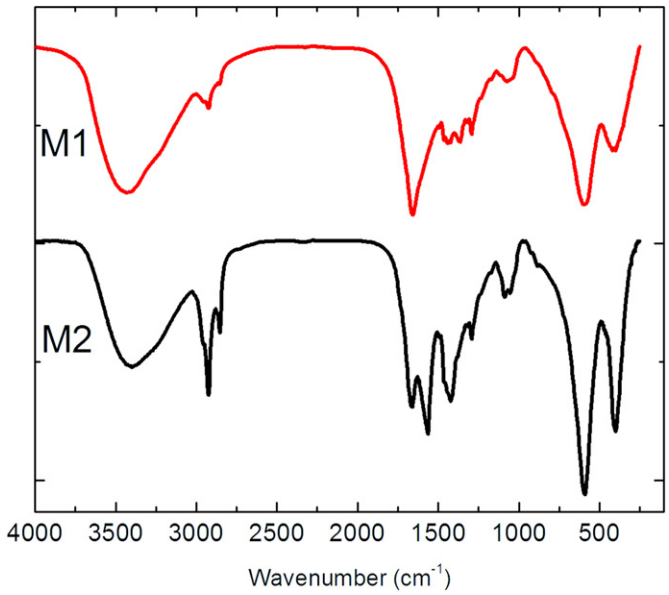

Fig. 1. FTIR spectra of M1 and M2 $CoFe_2O_4$/CS hollow spheres.

3.2. X-ray powder diffraction (XRD)

XRD patterns of the samples M1 and M2 in the Fig. 2 show the formation of ferrite structure and reveal that all peaks correspond to the characteristic peaks of cubic spinel type lattice of $CoFe_2O_4$ (JCPDS le No. 22-1086). The sample M1 show very broad peaks, indicating the ultra ne nature of these nanoparticles. The XRD spectrum of chitosan is reported in various literature [14] which shows peaks with low intensity values around $2\theta = 25°$ as it was shown for the M1 sample.

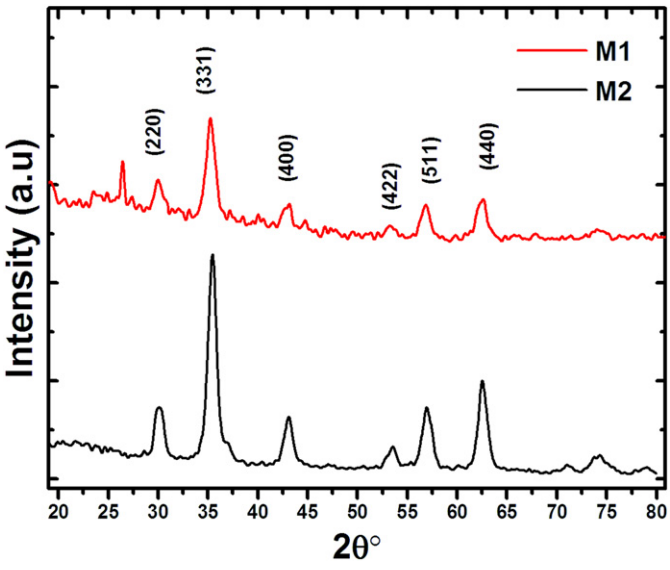

Fig. 2. X-ray powder diffraction patterns of M1 and M2 $CoFe_2O_4$/CS hollow spheres.

3.3. Thermogravimetric analyses (DSC - TGA)

For better understanding the physical and chemical changes that may have occurred during the formation of the $CoFe_2O_4$/CS hollow spheres, thermogravimetric analysis was performed. Thermogravimetric curves and its derivative (DSC) of M1 and M2 samples are displayed in Fig. 3. This figure shows three stages of weight losses in the DSC graph. The first stage occurred between 30 and 160 °C that is associated with the removal of water. The maximum rate of this process occurs at 63 °C. Then the chitosan begin to degrade at about 230 °C and the temperature of final decomposition is around 500 °C, the weight loss is significant (68%). The third, mass loss stage occurs around 600 °C in both samples and could be associated with the conversion of $CoFe_2O_4$ to CoO, which are the stable phase [15,16].

3.4. Energy dispersive X-ray analysis (EDX)

The objective of performing EDX analysis on the samples was to investigate the elemental composition. The data of elemental analysis of the $CoFe_2O_4$/CS hollow spheres are shown in the Table 1. Quantification of the EDX spectrum for the sample M2 showed that the ratio of Co, Fe, and O was about 1:2:4, suggesting that the hollow spheres had a chemical formula of $CoFe_2O_4$ and no contamination elements are detected.

3.5. SEM and TEM

SEM and TEM images of the samples M1 and M2 are shown in the Fig. 4. Fig. 4a shows the $CoFe_2O_4$ NPs obtained in situ by the solvothermal reaction with a ferrous precursor. The average particle size distribution obtained from TEM show that the mean size of the

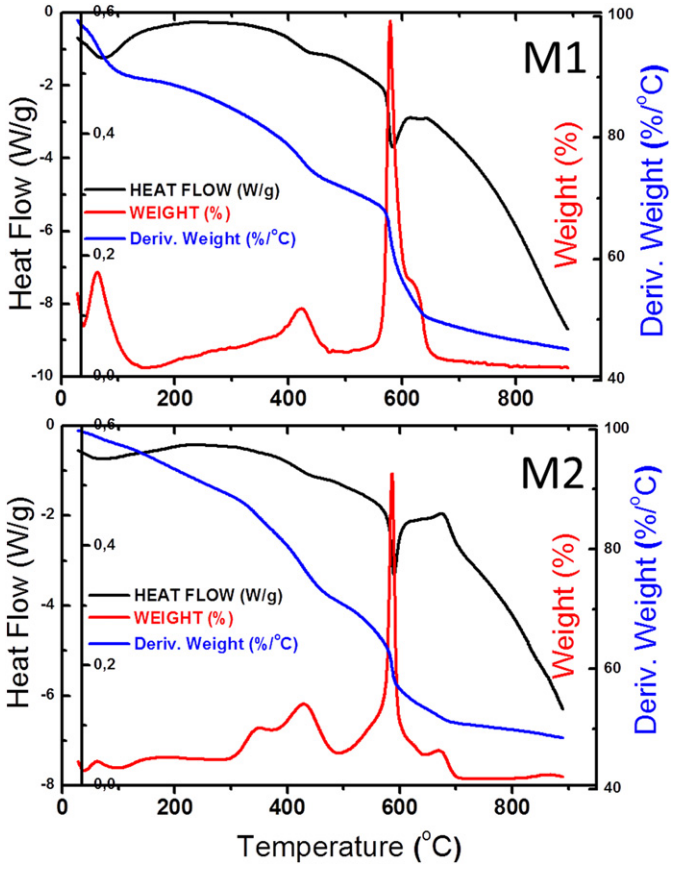

Fig. 3. Thermogravimetric analysis (DSC - TGA) of M1 and M2 $CoFe_2O_4$/CS hollow spheres.

Table 1
Elemental analysis of M1 and M2 $CoFe_2O_4$/CS hollow spheres.

Element	Atomic %	
	M1	M2
Co(K)	0.40	0.85
Fe(K)	2.12	2.03
O(K)	18.47	28.85
C(K)	79.01	68.63

NPs ranges from 4 ± 2 nm, with irregular shapes and agglomerated. At the synthesis conditions used, excessive alkali induces the Fe^{+2} and Fe^{+3} ions hydrolyzing faster, leads to nanoparticles rapidly changing into larger sized clusters with arbitrary smaller shaped nanoparticles. In the Fig. 4b we observe the morphology like spheres of the $CoFe_2O_4$ nanoparticles obtained using the thermal decomposition method without and with chitosan. The average particle size distribution obtained from TEM shows that the mean size of the NPs ranges from 6 ± 2 nm and the NPs are uniform in size and morphology. Fig. 4c and d reveals that each hollow sphere it is composed of aggregates of more primary nanoparticles. The general morphology of the samples observed by SEM and typical images at different magnifications are shown in Fig. 4e and f, it was observed that the major morphological feature is a regular spherical shape with an average particle diameter of about 100 nm. The high magnification SEM image (Fig. 4f) reveals the hollow interior of the sphere. The thickness of the shell consisting of the hollow spheres is about 40 to 50 nm.

3.6. Magnetic measurements (VSM)

Fig. 5 shows the magnetization versus applied field curves obtained for the samples M1 and M2 at room temperature. The remanent magnetization (1.6 and 3.8 emu/g) and coercivities (4.3 and 7.3 mT) obtained for the samples correspond to very soft ferromagnetic materials with a small response to the external magnetic field. The results shows the maximum magnetization (Mm) obtained for the sample M2 (28.9 emu/g) compare with the sample M1 (15.6 emu/g), attributed to the greater degree of crystallinity (Fig. 2), the uniform morphology and best dispersion behavior of the nanoparticles (Fig. 3). The irregular morphology of the sample M1 (Fig. 3a) might influence the value of Mm as a contribution from surface anisotropy. As the sample M2 (Fig. 3b) is almost spherical in shape, a zero contribution from surface anisotropy must be expected. A further reduction of Mm in the sample M1 could be attributed to incomplete crystallization of the ferrite after the reaction synthesis [17]. The better dispersibility with more uniform shapes of nanoparticles leads to more ordered inner magnetic vector, and so the stronger magnetic behavior [18]. The above results demonstrate that maximum magnetization of the hollow spheres is greatly influenced by dispersion properties of the NPs in the hollow sphere.

4. Conclusion

In summary, cobalt ferrite $CoFe_2O_4$/CS hollow spheres have been successfully synthesized using $CoFe_2O_4$ NPs formed in situ and ex situ on the solvothermal method. The prepared hollow spheres exhibit spherical morphology with a narrow size distribution. Magnetic properties are in influenced greatly by dispersibility and shape of particles. $CoFe_2O_4$/CS hollow spheres synthesized using $CoFe_2O_4$ NPs formed ex situ exhibit superior structural and magnetic properties. This approach can be an efficient route to fabricate cobalt ferrite spheres in large scale. The advantage of the present work is that the magnetic properties of the hollow spheres can be optimized by controlling the size of the nanoparticles formed previously by the thermal decomposition method.

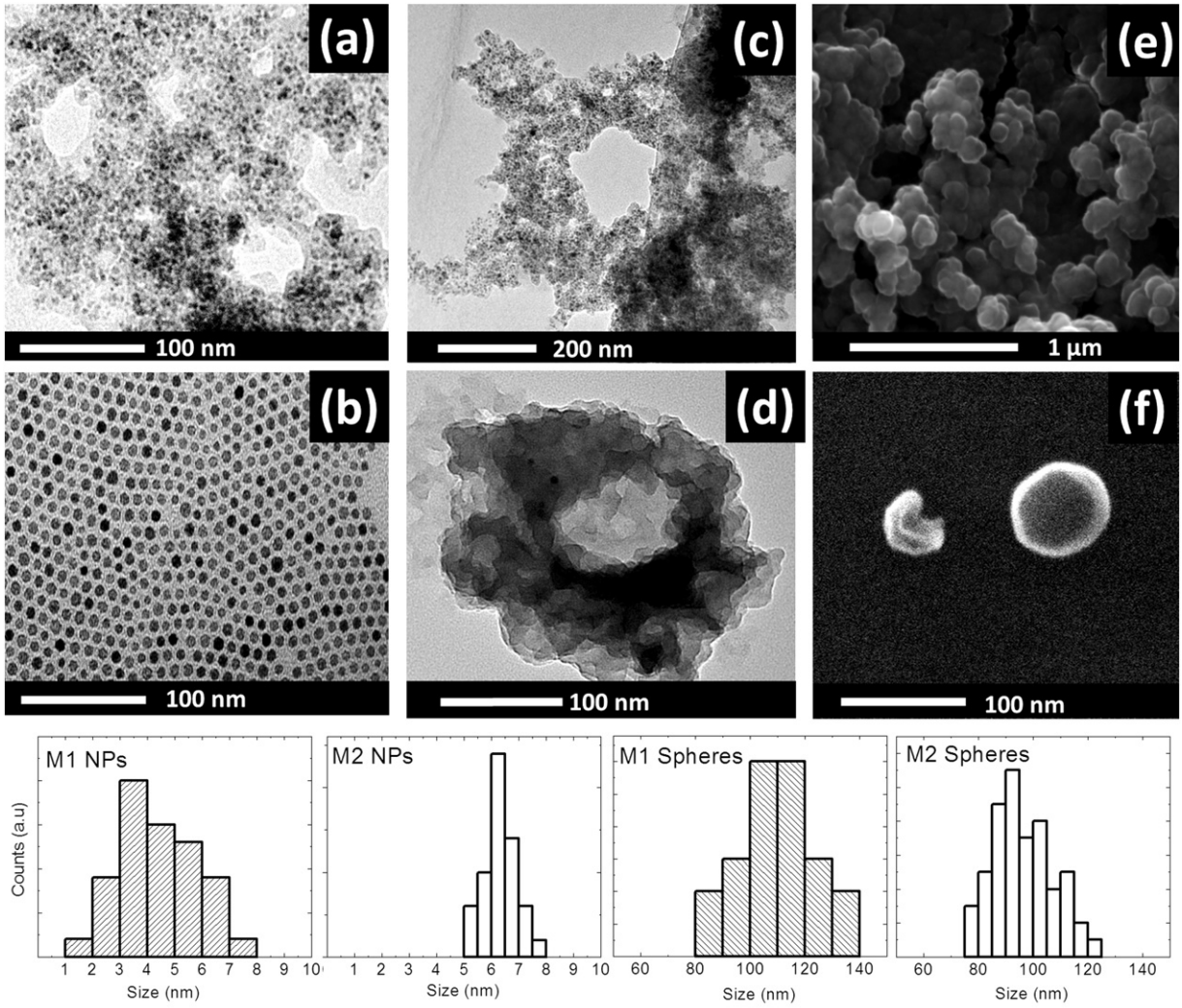

Fig. 4. TEM images of the (a) In-situ, (b) Ex-situ $CoFe_2O_4$ nanoparticles, (c) M1, (d) M2 $CoFe_2O_4$/CS hollow spheres. SEM images of the (e) M1, (f) M2 $CoFe_2O_4$CS hollow spheres. Average particle size distribution.

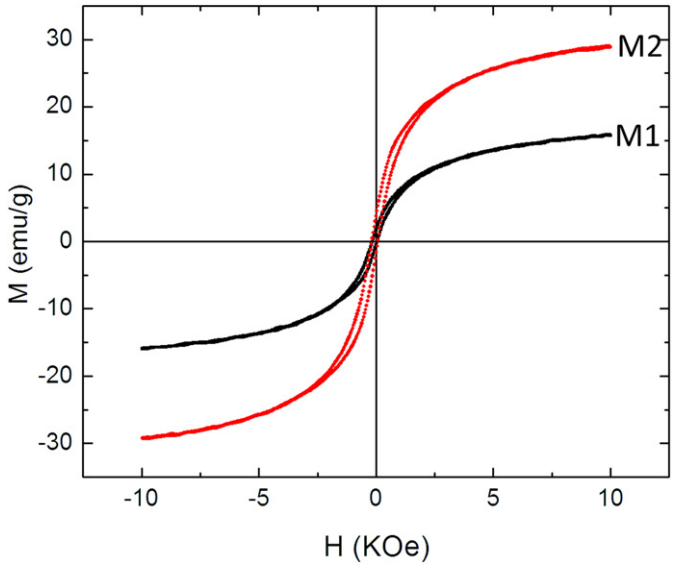

Fig. 5. Magnetization versus applied field at room temperature of M1 and M2 $CoFe_2O_4$/CS hollow spheres.

Acknowledgements

We thank to the Electron Microscopy Unit in the Chemistry Center IVIC for the TEM observation. Lisbeth Lozada and Josebas Echebarrieta for their support in sample preparation and SEM observation, Damarys Soto and Maria Elena Gomez for the IR-FT and TGA analyses.

References

[1] J. Wu, W. Jiang, Y. Shen, W. Jiang, R. Tian, Mater. Sci. Eng. C. 70 (2017) 132–140.
[2] Qi Lian, Z. Xue-Fang, H. Tie-Feng, Russ. J. Phys. Chem. A 89 (11) (2015) 2132–2136 (2015).
[3] I. Sharifi, H. Shokrollahi, S. Amiri, J. Magn. Magn. Mater. 324 (2012) 903–915.
[4] Z. Weifeng, Xuelian Huang, Yilin Wang, Shudong Sun, Chang-sheng Zhao, Carbohydr. Polym. 150 (5) (2016) 201–208.
[5] S. Briceño, W. Bramer-Escamilla, P. Silva, J. Magn. Magn. Mater. 324 (18) (2012) 2926–2931.
[6] S. Sun, H. Zeng, D.B. Robinson, S. Raoux, P.M. Rice, J. Am. Chem. Soc. 126 (2004) 273–279.
[7] M. Shen, Y. Yu, G. Fan, Nanoscale Res. Lett. 9 (2014) 296.
[8] Z. Li, M. Lai, X.Y. Wang, D. Mao, J. Phys. Chem. C 113 (7) (2009) 2792–2797.
[9] G. Unsoy, S. Yalcin, J. Nanopart. Res. 14 (2012) 964.
[10] M. Mandal Goswamia, C. Deya, A. Bandyopadhyay, D. Sarkara, M. Ahirb, J. Magn. Magn. Mater. 417 (2016) 376–381.
[11] K. Donadel, M.D.V. Felisberto, V.T. Fvere, M. Rigoni, N. Jhoe Batistela, M.C.M. Laranjeira, Mater. Sci. Eng. C 28 (2008) 509–514.
[12] W. Zou, H. Geng, M. Lin, X. Xiong, J. Appl. Polym. Sci. 123 (2012) 3587–3594.

[13] B. Wang, P.P. Zhang, G.R. Williams, B.W. Christopher, J. Quan. J. Mater. Sci. 48 (2013) 3991–3998.
[14] T. Aziz, S. Md, Md Masum, Rakibul Qadir A. Gafur, D. Huq, Int. Res. J. Pure. Appl. Chem. 11 (1) (2016) 1–9.
[15] M. Ziegler-Borowska, D. Cheminiak, H. Kaczmarek, J. Therm. Anal. Calorim. 119 (2015) 499–506.
[16] P. Soares, Diana Machado, Cesar Laia, Laura C.J. Pereira, Joana T. Coutinho, Isabel M.M. Ferreira, Carlos M.M. Novo, Joao Paulo Borges, Carbohydr. Polym. 149 (20) (2016) 382–390.
[17] M. Mascolo, Y. Pei, Materials 6 (2013) 5549–5567.
[18] X. Liang, H. Shi, et al., Mater. Sci. Appl. 2 (2011) 1644–1653.